J. Water Environ. Nanotechnol., 8(1): 41-51 Winter 2023

ORIGINAL RESEARCH PAPER

Immobilized nickel hexacyanoferrate nano particles on graphen for effective removal of Cs(I) ions from radionuclide wastes.

Noorallah Delijeh [1], Taher Yousefi [2], Hassan Aghayan [2,*], Ramin Yavari [2],Mehdi Parvini [1], Hossein Ghasemi Mobtaker [2]

[1] *Department of Chemical Engineering Gas and Petroleum, Semnan University, 35196-45399, Semnan, Iran*
[2] *Nuclear Fuel Cycle Research School, Nuclear Science and Technology Research Institute, Tehran, Iran*

Received: 2022-10-28 Accepted: 2023-01-06 Published: 2023-02-11

ABSTRACT

In the current work, the synthesis and modification of graphene oxide with Nickel Hexa Ferrocyanide (NiHCF) nanoparticles has been reported.

The obtained product was characterized and used as an adsorbent to remove Cesium (Cs) ions from a simulated solution. Studying the Cs uptake in various pHs indicated that it reaches about 99% at a pH range of 6-7. The results cleared that the maximum adsorption for Cs was 240 mgg^{-1}. Equilibrium modeling studies suggest that the data are reasonably and relatively fitted well to the Langmuir adsorption isotherm. Kinetic studies show that the sorption process is fairly rapid and equilibrium is achieved at an initial 30 min of contact time, as well the kinetic data are fitted well to the pseudo-second-order rate mode.

Keywords: Cesium(I); Nickel Hexa Ferrocyanide; Nanoparticles; Graphen Oxide; Adsorption; Adsorption Capacity; Nuclear waste

How to cite this article

Delijeh N., Yousefi T., Aghayan H.,Yavari R., Parvini M., Ghasemi Mobtaker H., Immobilized nickel hexacyanoferrate nano particles on graphen for effective removal of Cs(I) ions from radionuclide wastes. J. Water Environ. Nanotechnol., 2023; 8(1): 41-51 DOI: 10.22090/jwent.2023.08.005

INTRODUCTION

The operation of nuclear power plants as an alternative source to conventional coal thermal power plants has increased worldwide and it is causing greatly the occurrence of high levels of radioactive wastes [1-2]. Radioactive Cs-137 ion is a significant component of nuclear waste and the nuclear fallout which would be produced during the operation of uranium reactors. This radioisotope is highly radiotoxic and has a long half-live (30.17 yrs), and needs to be separated from the waste during the management of radioactive wastes.

To avoid the entrance of even a slight value of Cs ion to the environment, unlike the other wastes, proper and careful handling of the radioactive waste is necessary [1-2]. Various methods including reverse osmoses, evaporation/ concentration, coagulation, flocculation, co-precipitation, ion exchange, adsorption, and biological methods, have been used for the removal of Cs(I) from aqueous wastes. However, some of these methods have serious limitations in waste treatment. For example, if the cesium is in soluble form, conventional coagulation processes exhibit negligible Cs removal. Thus the development of a cost-effective and efficient Cs removal process is vital. Adsorption of cesium by various adsorbents from aqueous solutions in batch and continuous operations is a promising process of cesium removal and was described in detail by numerous academic publications [3-5].

Due to the radiation stability and high ion-exchange capacity, many inorganic cation exchangers, such as clay minerals, zeolites, poly oxometalates, and metal oxides have been already

* Corresponding Author Email: *haghayan@aeoi.org.ir*

studied for the removal of radioactive cesium from nuclear wastewater. However, most of these adsorbents suffer from low capacity and selectivity.

Hexacyanoferrates (II) and - (III) of several transition metals have a high selectivity and capacity for cesium uptake over wide pH ranges and good resistance to ionizing radiations [6]. Nickel ferrocyanides are an example of them with a face-centered cubic structure that can selectively adsorb alkali cations. Since the cubic lattice size in Nickel ferrocyanides is similar to that of cesium ions, Nickel ferrocyanides can selectively adsorb Cs compared to other alkali cations.

Besides the good selectivity and capacity of metal ferrocyanides for cesium ions, these compounds have a deficiency that is associated with their nano or micrometer size that makes them available as a fine powder, with low chemical and mechanical stability [7].

Aggregation of fine powder leads to the decrease of metal ferrocyanides surface area and as a result the contact surface which decreases removal capacity and causes extremely high-pressure drop or head loss in fixed-bed column operation. These are not suitable for any flow-through systems and subsequently, reduce their effectiveness. To overcome this problem the immobilization on or impregnation in a suitable matrix is essential.

Graphene, a type of two-dimensional nanomaterial consisting of sp^2-hybridized carbon, has been considered an ideal substrate for the immobilization of metal ferrocyanides because, of its extremely high theoretical surface area (2630m^2 g^{-1}) and high affinity for metals adsorption [8–11]. Its derivative, graphene oxide (GO), has many functional groups (–O–, –OH, and –COOH) on its surface. These functional groups could combine with heavy metal ions to form strong complexes [12–18]. The graphene delivers a high surface area for the immobilization of NiHCF nanoparticles which leads to an increase in the contact surface of NiHCF nanoparticles with media and increases the sorption capacity. Also, the impregnation of NiHCF nanoparticles on graphene layers leads to enhancing the chemical and mechanical properties of a composite. In other words, the immobilization of NiHCF nanoparticles on graphene sheets prevents the agglomeration of a nanoparticle. A synergistic effect is concluded between the high surface area of graphene and the high selectivity and capacity of NiHCF nanoparticles which led to enhancing the adsorption performance of the composite. Herein, we demonstrate an in situ co-precipitation strategy to prepare the NiHCF nanoparticles supported on the graphene oxide (GO), and its usage for effective uptake of Cs(I) from nuclear waste.

MATERIALS AND METHODS

Materials and Apparatus

All materials were of analytical reagent grade and used as received without any further modification. The solutions were prepared with distilled water. H_2SO_4 (98%), $NaNO_3$, $KMnO_4$, HCl (37%), $NiCl_2.6H_2O$, $K_3[Fe(CN_6)].3H_2O$, $Cs(NO_3).6H_2O$, HNO_3 (63%), NaOH, and H_2O_2 were obtained from the Merck.

The Graphene Oxide and composite were specified by scanning electron microscopy (SEM, [LEO 1455VP]), X-ray diffraction (XRD, Phillips, PW-1800) equipped with monochromatized CuKα radiation (k = 0.154 nm, 40 kV and 30 mA). Fourier transform infrared (FTIR) of the samples was recorded by a KBr pellet on a VECTOR-22 (Bruker) spectrometer ranging from 400 to 4000 cm^{-1}. Thermogravimetric analysis (TGA) was performed on a thermobalance (PL-STA 1500, PL Thermal Science). The Cs(I) concentration in the solution was determined by Atomic Absorption Spectroscopy(AAS).

Preparation of Graphene Oxide(GO)

To synthesize, Graphene oxide, Hummer's method was used [19, 20], in which graphite powder was used as a starting material.

In this method, 140 ml of sulfuric acid (H_2SO_4) was added to the beaker in an ice bath and stirred for several minutes. Then 2 g of graphite powder and 1 g $NaNO_3$ were added to the mixing solution under stirring conditions. 6 g of potassium permanganate ($KMnO_4$) was then added slowly into the solution. This mixture was stirred for 2 hours out of an ice bath at 60°C and 100 ml water was added slowly. To eliminate the excess $KMnO_4$, 1-1.5 ml of hydrogen peroxide (H_2O_2) was dropped slowly and stirred for 10 minutes. The exothermic reaction occurred and then it was allowed to cool down. 100 ml of deionized water (DIW) was added and the mixture was settled for 12 h. Then, the supernatant was decanted away and the residuals were washed with DIW. Then 27 ml HCl (10 %) was added to GO, stirred for several minutes, and then washed with DIW. The washed GO was dried in an oven at 60 °C for 24 hours to produce the GO powder.

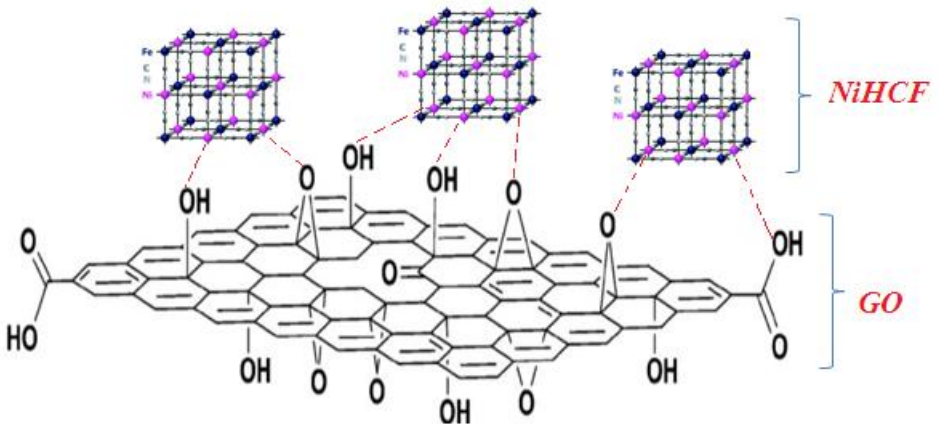

Scheme1; Immobilized Nickel hexacyanoferrate on a graphene sheet

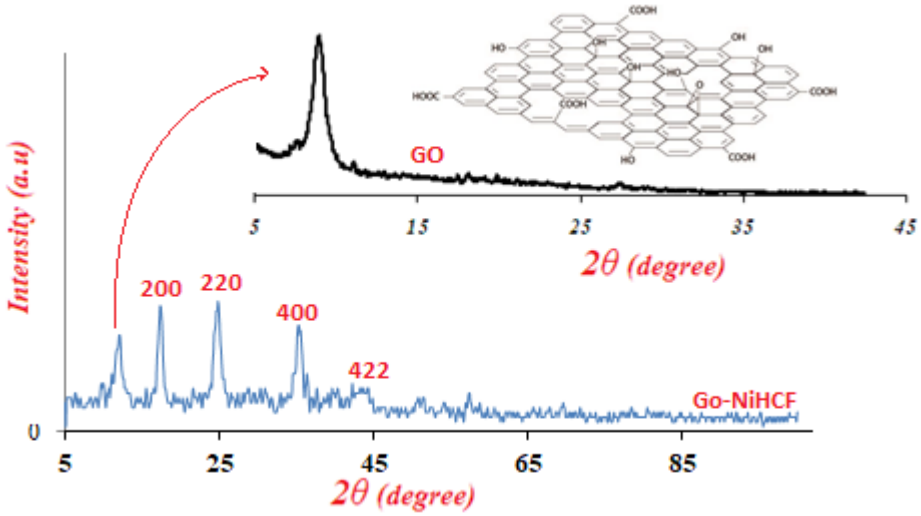

Fig.1 XRD pattern of GO-Nickel hexacyanoferrate and GO (inset) samples (at 25 °C and 24 hours)

Preparation of nickel hexacyanoferrate immobilized on Graphene (NiHCF-G)

The immobilization of Nickel hexacyanoferrate was carried out in two steps. In the first step, the Ni^{2+} was loaded on graphene oxide, and secondly, it was converted to potassium nickel ferrocyanide (scheme1). To produce graphene oxide - Nickel hexacyanoferrate, 3 g of GO was added to a solution of 1 M Nickel chloride ($NiCl_2.6H_2O$) and was shaken (200 rmp) at 25 °C for 24 hours. Then the GO was washed with DIW for the removal of excess Nickel chloride. The sample was dried in an oven at 60°C for 24 h. The Ni^{2+}-GO sample was added to a solution containing 1 M ferrocyanide and stirred for 24 h at 30°C. Then residual was rinsed with DIW.

Adsorption

The sorption behavior of the GO- Nickel hexacyanoferrate sample for Cs (I) ions were determined in batch mode. The effect of various factors including time, initial concentration, adsorbent dosage, and temperature, which evaluate the sorption ability of the sample, were studied. The experiments were conducted using 0.1 g of adsorbent with 20 ml of solutions containing Cs (I) ions of the desired concentrations at different temperatures with continuous stirring at 600 rpm. After shaking, the solid phase was separated from the solution by filtration, and then the concentration of Cs (I) was determined in the liquid phase using atomic absorption spectrometry

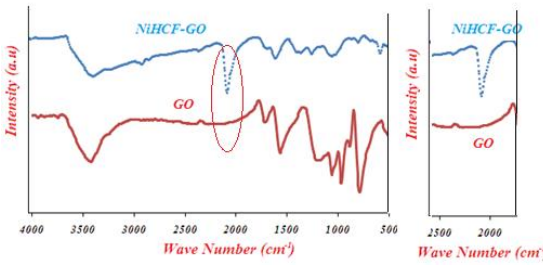

Fig. 2 FTIR spectra of GO and GO-NiHCF samples

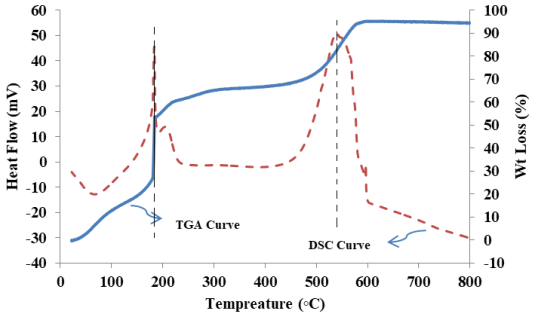

Fig. 3 TGA and DSC curves of GO-Nickel hexacyanoferrate sample.

(AAS). The solution of 0.1 M KOH or 0.1 M HNO_3 was used to adjust the solution pH. To obtain the sorption capacity, the number of ions adsorbed per unit mass of adsorbent was evaluated according to the following expression (1):

$$Q_e = (C_i - C_e)\frac{V}{W} Q_e = (C_i - C_e)\frac{V}{W} \quad (1)$$

Where Q_e is milligrams of adsorbed metal ions per gram of adsorbent,V (L) is the volume, C_i and C_e (mg L^{-1}) are the initial and final solution concentrations of metal ions respectively, and w (g) is the dry mass of the solid. The adsorption percentage of metal ions was calculated as follows:

$$\text{Adsorption}(\%) = \frac{C_i - C_e}{C_i} \times 100 \quad (2)$$

RESULTS AND DISCUSSION

Characterization of the sample

XRD

The XRD pattern of synthesized GO (inset) and GO-Nickel hexacyanoferrate samples is shown in Fig. 2. The diffraction peak around 10 °(2θ), in GO (inset) and GO-Nickel hexacyanoferrate patterns, is mainly due to the oxidation of graphite and its successful transformation to graphene oxide. The diffraction peak of pure graphite is around 26°, which is disappeared in the patterns and shows that the product is completely oxidized [21]. From the XRD pattern of GO-Ni-HCF, the peaks at 2Θ =17.14°, 24.70°, 35.40°, and 43.50°, correspond to the (200), (220), (400), and (422) planes of Ni-HCF, respectively (JPCDS No. 46-0906) [22]. All diffraction peaks of Ni-HCF can be perfectly indexed as cubic nickel iron cyanide hydrate. The lattice parameters of Ni-HCF are $a = b = c = 10.23$ Å and $\alpha = \beta = \gamma = 90°$. The space group of Ni-HCF is F-43 m (216). Therefore, the immobilization of Nickel hexacyanoferrate on graphene oxide was confirmed by XRD.

FTIR

Fig. 2 shows the FTIR spectra of synthesized GO and GO-Nickel hexacyanoferrate samples. Both spectra show a broad peak at 3000-3700 cm^{-1} which is due to the stretching vibration of hydroxyl groups (OH) of graphene oxide. The peaks at 1600 cm^{-1} and 1720 cm^{-1} are due to the stretching vibration of C=C and C=O of carboxylic groups present at the edges of GO. Further, the peaks at 1187 cm^{-1} and 1064 cm^{-1} correspond to the C-O of carboxylic acid and C-OH group of alcohol, which ensures that the oxygen-containing functional groups are present there and graphene has been completely oxidized. For GO-Nickel hexacyanoferrate spectra, a sharp peak at 2090 cm^{-1} is an indication of the C≡N group and it confirms the presence of nickel ferrocyanide on the Graphene oxide [23,24].

TGA

The thermal stability of the GO-Nickel hexacyanoferrate sample was studied by TGA and DSC.

The TGA and DSC curves of the GO-Nickel hexacyanoferrate sample in the range of 25–800 °C and a heating rate of 10 °C min^{-1} under air atmosphere are shown in Fig. 3. As can be seen from the thermogram and DSC curves, three steps of weight loss take place during continues heating of the sample. The first step starts at about 90 °C and continues until 190 °C which can be attributed to the removal of adsorbed and coordinated water (see the corresponding small endothermic peak in the DSC curve). The second significant weight loss is observed at around 200 °C, due to the decomposition of the oxygen-

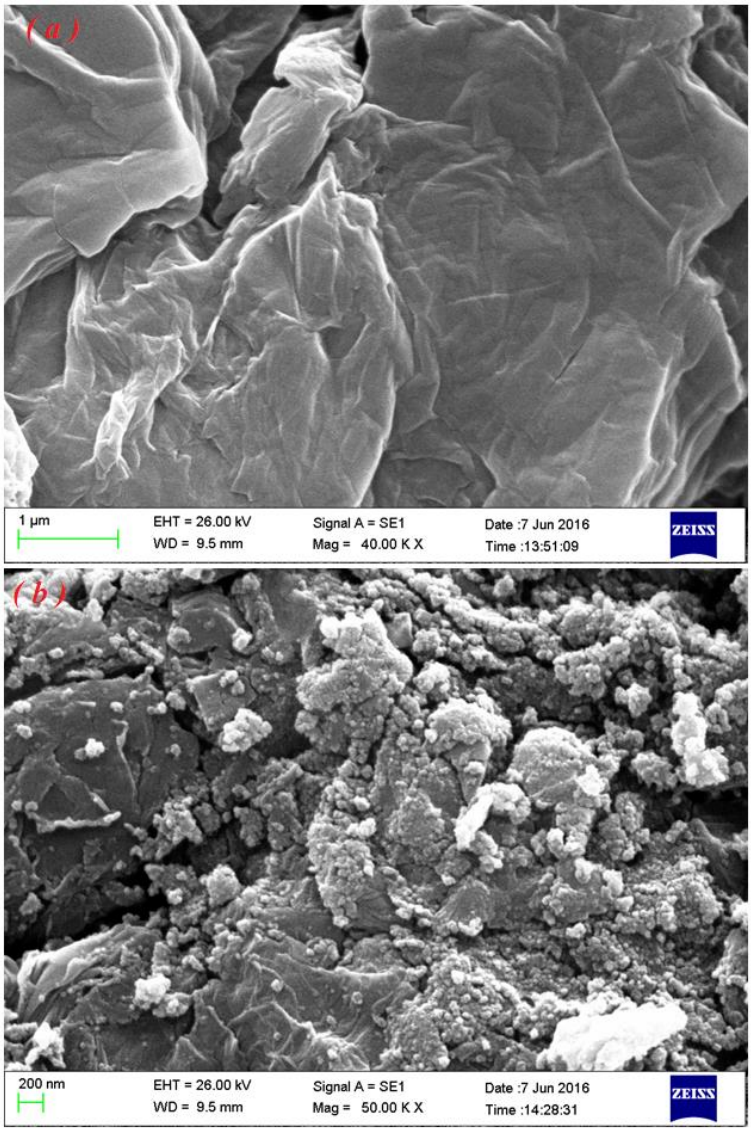

Fig. 4 SEM images of graphene (a) before and (b) after immobilization of NiHCF

containing functional groups, and incomplete pyrolysis of the carbon skeleton of GO, yielding CO, CO_2, and steam (see also the corresponding sharp exothermic peak in the DSC curve). The third step weight loss which starts at about 550 °C (see also the corresponding sharp exothermic peak in the DSC curve) is due to the complete pyrolysis (decomposition and burning of graphene) of the sample.

SEM

The morphology of GO and GO-NiHCF samples was studied by SEM (Fig. 4a and b). Fig. 4a shows the graphene sheet image before the immobilization of NiHCF nanoparticles. As can be seen, the GO sheets were prepared with smooth and planar surfaces containing some wrinkles. Fig 4b shows the graphene sheet after immobilization of NiHCF nanoparticles. As can be seen, nanoparticles ranging from 40-80 nm are disturbed on the graphene sheet, and somewhere agglomeration of nanoparticles leads to the formation of larger particles. The SEM images indicated that the surface morphology of the graphene sheets was changed significantly with the immobilization of nickel hexacyanoferrate.

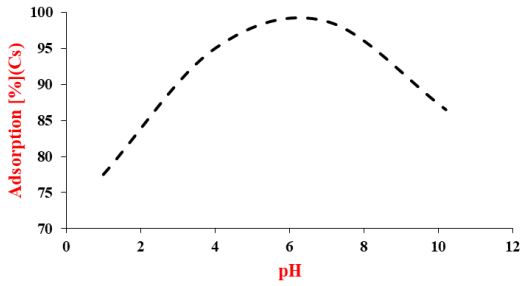

Fig. 5 The effect of pH (1, 4, 7, and 10) on Cs(I) uptake by GO-NiHCF at 20 mgL^{-1} and 25 °C with continuous shaking at 150 rpm for 5 h.

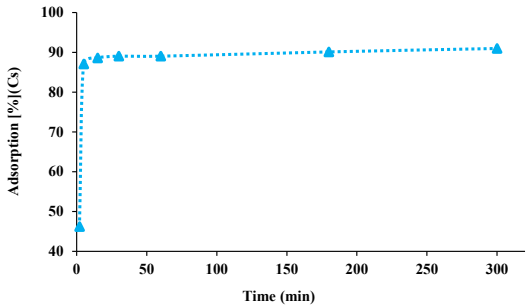

Fig. 6 The effect of contact time (10-300 min) on Cs(I) uptake, at 25°C and pH 7 with continuous shaking at 150 rpm

Adsorption

pH effect

The pH is an effective parameter in metal uptake from the aqueous solution. During the change of solution pH, the surface charge of the adsorbents may be affected or the adsorbate ions speciation or precipitation may be taken place or competitor ion concentration may be changed. Solutions of HNO_3 and KOH were used for pH adjustments. The effect of pH on Cs uptaking of the GO-NiHCF sample, was determined in the range of 1-10 (Fig. 5). Batch adsorption experiments were done using 0.05 g of GO-NiHCF with 20 ml of solutions containing Cs(I) ions of 20 mgL^{-1} at various pHs (1, 4,7 and 10) in 50 ml plastic bottles with continuous shaking at 150 rpm for 5 h. Then the mixture was filtrated and the obtained solution was analyzed for Cs(I) ions with AAS. As can be seen by increasing the pH, the Cs uptake by GO-NiHCF increases and reaches about 99% at pH 7. At low pHs, decreasing Cs(I) uptake is due to the dissolution of a portion of sorbent or competition of H^+ for sorbent sites. At pHs greater than 7, the Cs hydroxides began to form and some of them were negatively charged $Cs(OH)^{2-}$ which resulted in a decrease of Cs uptake due to the electrostatic repulsion [25].

Effects of contact time and adsorption kinetics

To determine and optimize the equilibrium time of Cs(I) uptake by GO-NiHCF sample,

the effect of contact time at 25°C and pH 7 was investigated. The removal percent of Cs(I) by GO-NiHCF as a function of adsorption time is shown in Fig. 6. As can be seen, the initial uptake rate of Cs(I) was very fast and slowed down by time[26] and an apparent equilibrium is achieved within 30 min of contact time. The fast uptake of ions and achievement of equilibrium at the initial contact time can be attributed to the large Cs(I) ions concentration gradient between the GO-NiHCF and the solution. Then due to the occupation of more sorption sites, the uptake slowed down [25, 27].

The results of the cesium removal by the GO-NiHCF were tested in pseudo-first-order, pseudo-second-order, Morris–Weber, and Elovich kinetics models.

The pseudo-first-order kinetic model is the most widely used equation describing the adsorption rate of adsorbate from a liquid phase. It is represented as [28]:

$Ln(q_e-q_t) = Lnq_e-K_1t$(3)

where q_e and q_t are the amounts of the ions adsorbed ($mg{\cdot}g^{-1}$) on the adsorbent in equilibrium and at time t, respectively, and K_1 (min^{-1}) is the rate constant of the adsorption.

According to Eq.(3), (q_e) and (K_1) parameters can be individually calculated from the slope and intercept of the plot of $Ln(q_e-q_t)$ versus time.

The kinetics of the sorption was also described by the pseudo-second-order rate model. This model is expressed as [29]:

$$\frac{1}{q_e - q_t} = \frac{1}{q_t} + k_2 t \quad (4)$$

$$\frac{t}{q_t} = \frac{1}{k_2 q_e^2} + \frac{1}{q_e} t \quad (5)$$

where k_2 is the rate constant of the pseudo-second-order equation (g/mg min).

If the initial sorption rate h (mg L^{-1} h) is:

$$h = k_2 q_e^2 \quad (6)$$

then Eqs. (5) and (6) become:

$$\frac{t}{q} = \frac{1}{h} + \frac{1}{q_e} t \quad (7)$$

Table 1. Kinetic parameters for Cs(I) sorption by GO-NiHCF (contact time interval 10-300 min, at 25°C and pH 7 with continuous shaking at 150 rpm)

Kinetic models		
	k_1 (min^{-1})	0.0108
The pseudo first-order model	q_e($mg\ g^{-1}$)	33.84
	R^2	0.5094
	k_2 (g/mg min)	0.044
The pseudo second-order model	q_e($mg\ g^{-1}$)	33.784
	R^2	0.999
	k_{id} ($mg/g\ min^{-1/2}$)	0.0631
Intraparticle diffiusion	Intercept (C)	32.709
	R^2	97.48
	$\alpha(mg/g\,\min)$	$>10^3$
Elovich model	β ($mg\ g^{-1}$)	1.026
	R^2	0.599

The kinetic plot of t/q_t versus t for ions sorption is used for parameter extraction, and the correlation coefficient (R^2) suggests a correlation between the parameters and experimental data.

The intraparticle diffusion model is expressed as [29]:

$$q_t = k_{ad}t^{1/2} + c \quad (8)$$

Where k_{ad} is the rate constant of intraparticle transport ($mg/g\ min^{1/2}$), and c is the boundary layer diffusion. According to this model, plotting a graphic of q_t versus $t^{1/2}$, in the light of a straight line with intercept c, can pave the way for the assumption that the involved mechanism is a diffusion of the species.

The kinetics of the sorption was also described by the Elovich model. This model describes the uptake rate on the adsorbent decreases exponentially with an increase in the amount of the adsorbed material [30]: This model is represented by the following equation

$$dq/dt = ae^{-\alpha q} \quad (9)$$

Where q represents the number of ions adsorbed at time t, "a" the desorption constant, and "α" the initial adsorption rate.

The kinetic parameters for four kinetic models and correlation coefficient (R^2) were calculated as listed in Table 1. These data, evidently disclose that the correlation coefficient (R^2) has a high value and is closer to unity for the pseudo-second-order kinetic model than the other kinetic model, thus clarifying the matching of the experimental data with the pseudo-second-order kinetic model.

Effect of concentration

The Cs (I) solutions with different concentrations of 50, 100, 250, 500, 1000, and 2000 mg L^{-1} were used for the adsorption isotherm investigation. The experiments were carried out by varying the initial concentration at constant pH of 7.0 and temperature of 25 ◦C. A driving force would be provided by initial concentration to overcome the mass transfer barrier in the aqueous and the solid interface. Therefore, in general, by increasing the sorptive concentrations the sorption is favored.

The equilibrium state sorption data are plotted with the amount of Cs(I) sorbed ($mg\ g^{-1}$) versus the initial concentration of Cs(I) in Fig. 9a. As can be

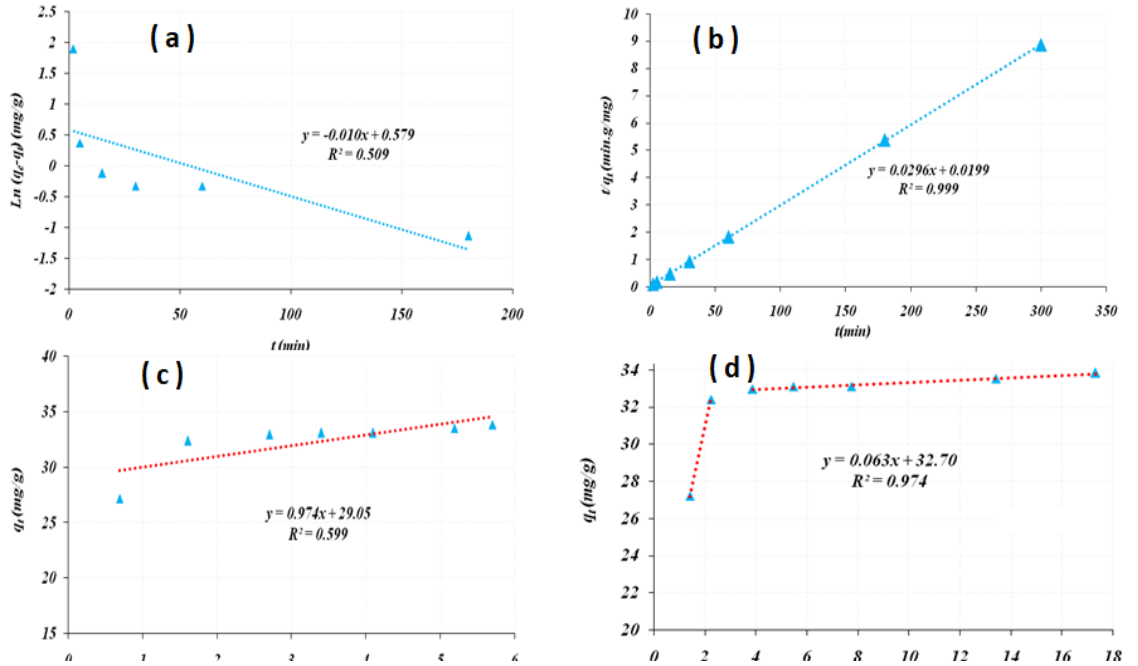

Fig.7. straight-line plots of (a) pseudo-first-order, (b) pseudo-second-order, (c) Elovich, and (d) Morris–Weber kinetic model applied to the uptake of Cs(I) by GO-NiHCF.

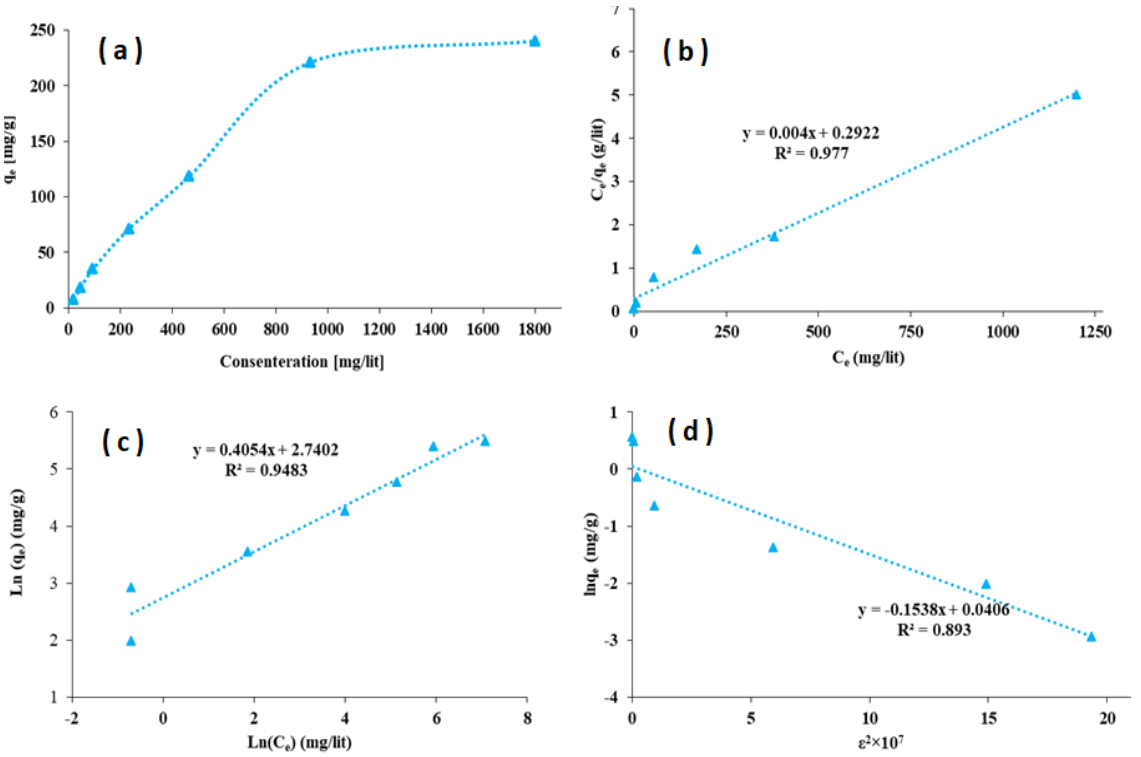

Fig. 8. (a) uptake of Cs(I) at various initial concentrations,(b)straight-line plot of Langmuir model, (c) straight-line plot of Freundlich model, (d) straight-line plots of Dubinin– Radushkevich model

Table 2. Sorption isotherm parameters of Cs(I) (at concentrations of 50, 100, 250, 500, 1000, and 2000 mg L-1 at constant pH 7.0 and temperature 25 ◦ C)

Isotherms		
Langmuir	q_m(mg g^{-1})	250
	K_L(L/mg)	0.0137
	R_L	0.0352
	R^2	0.977
Freundlich	K_F(mg g^{-1})	15.49
	n_F(L/mg)	2.47
	R^2	0.9483
Dubinin–Radushkevich	$q_{DR}(mmol/g)$	1/041
	$B_{DR}(mol^2/l^2)$	1/538E-8
	Ea(KJ/mol)	5/701
	R^2	0/893

seen at first, by increasing the initial concentration, an increase in the amount of Cs(I) uptake was observed, which becomes gradually constant with more increasing the initial concentration. The results indicated the high sorption capacity of about 250 mg g^{-1} was achieved at 1000 ppm, this suggests the potential applicability of GO-NiHCF for decreasing cesium concentration in contaminated water. The obtained sorption data at different Cs(I) concentrations were used for equilibrium modeling by Langmuir, Freundlich, and Dubinin–Radushkevich adsorption isotherms.

Langmuir model is a model for monolayer adsorption on a surface with a finite number of identical sites, which can be expressed as [31]:

$$C_e/q_e = 1/q_m K + C_e/q_m \quad (10)$$

Where q_m (mg g^{-1}), is the maximum removal capacity (monolayer), Ce is the equilibrium concentration of the metal ion in the equilibrium solution (mg L^{-1}), and K (L $mg^{\circ 1}$) is the Langmuir constant related to the free energy of adsorption ($b\circ e^{-\Delta G/RT}$). The q_m and K could be determined from the slope and intercept of the Ce/q_e vs. Ce curve

Freundlich adsorption equation as non-ideal and reversible adsorption in multilayer was taken as (Eq. (11)):

$$Ln(q_e) = Ln(K_F) + (1/n)\, Ln(C_e) \quad (11)$$

where C_e (mg L^{-1}) is the equilibrium concentration of ions, q_e (mg g^{-1}) is the amount of adsorbed ions, and n and K_F (mg g^{-1}) are the Freundlich constants related to the intensity of the adsorption and the sorption capacity respectively.

The Dubinin-Radushkevich (D-R) isotherm compared to the Langmuir isotherm, does not assume a homogeneous surface or constant sorption potential [32]. The D–R isotherm is as follows:

$$Lnq_e = Lnq_m - \beta\, \xi^2 \quad (12)$$

where q_m is the maximum uptake of ion by adsorbent (mmol/kg), βis a constant related to the sorption energy (mol^2/kJ^2); and ε is the Polanyi potential (RTln (1 + 1/Ce)), where R and T are the gas constant (kJ/mol.K), and the absolute temperature respectively. The ε is given by Eq.(13)

$$\varepsilon = RT \ln [1 + 1/C_e] \quad (13)$$

where C_e is the adsorbate equilibrium concentration (mg/L).

The adsorption isotherms of Cs(I) ions on the GO-NiHCF are shown in Fig 9 (b- d). The isotherms constants and the coefficients are given in Table 2.

The regression coefficient i.e., R^2 values in Table 2, indicate that the sorption of Cs(I) is best fitted to the Langmuir model. Langmuir model can give an insight into the maximum uptake capacity and indicates whether the sorption is favorable or not.

CONCLUSION

Graphene oxide was synthesized by Hummer's method and was modified with Nickel hexacyanoferrate nanoparticles. The obtained composite was characterized by XRD, FTIR, TGA, and SEM analyses and tested as an adsorbent for

the uptake of Cs(I) from aqueous solutions. The new sorbent showed good affinity to Cs (I) ions and showed a high adsorption capacity of 240 mg g^{-1}. The ion uptake characteristic was examined by the variations in the parameters of the initial concentration of the metal ions, pH, and contact time. The SEM images of the product showed that nanoparticles ranging from 40-80 nm are distributed on a graphene sheet and in somewhere agglomeration of nanoparticles leading to the formation of larger particles. Studying the effect of pH on adsorption, indicated that by increasing the pH, the Cs uptake by GO-NiHCF increases and reaches about 99% at pH 7. Kinetics studies clarified the matching of the experimental data by the pseudo-second-order kinetic model. The regression coefficient values indicated that the sorption of Cs(I) is best fitted to the Langmuir model. This adsorbent has effective removal properties for the adsorption of Cs(I) from the radioactive waste compared with other adsorbents.

CONFLICT OF INTEREST

The authors declare no conflict of interest.

REFERENCES

[1] Y. Seo , Y. Hwang, Prussian blue immobilized on covalent organic polymer-grafted granular activated carbon for cesium adsorption from water, Journal of Environmental Chemical Engineering, 9, (5)(2021) 105950 https://doi.org/10.1016/j.jece.2021.105950

[2] C. Lalhmunsiama, Lalhriatpuia, D. Tiwari, L. Seung-Mok, Immobilized nickel hexacyanoferrate on activated carbons for efficient attenuation of radio toxic Cs(I) from aqueous solutions, Applied Surface Science 321 (2014) 275-282 https://doi.org/10.1016/j.apsusc.2014.09.200

[3] M. Pipíška , S. Ballová , V. Frišták , L. Ďuriška , M. Horník , Š. Demčák , M. Holub and G. Soja, Potassium nickel(II) hexacyanoferrate(III)-functionalized biochar for selective separation of radiocesium from liquid wastes, JOURNAL OF RADIATION RESEARCH AND APPLIED SCIENCES, 13(1))2020) 343-355. https://doi.org/10.1080/16878507.2020.1740394

[4] J. Bu, R. Gonzalez Teresa, K. G.Brown, F. Sanchez, Adsorption mechanisms of cesium at calcium-silicatehydrate surfaces using molecular dynamics simulations. Journal of Nuclear Materials, 515 (2019) 35-51. https://doi.org/10.1016/j.jnucmat.2018.12.007

[5] K. L. Lee, S. H. Lee, J. E. Lee, S. Y. Lee, Biosorption of radioactive cesium from contaminated water by microalgae Haematococcus pluvialis and. Chlorella Vulgaris. Journal of Environmental Management, 233(2019) 83-88. https://doi.org/10.1016/j.jenvman.2018.12.022

[6] S. Ayrault, B. Jimenez, E. Garnier,- M. Fedoro, D. J. Jones, and C. Loos-Neskovic, Sorption Mechanisms of Cesium on CuII 2FeII(CN) 6 and CuII 3[FeIII(CN)6]2 Hexacyanoferrates and Their Relation to the Crystalline Structure, JOURNAL OF SOLID STATE CHEMISTRY 141 (1998). 475-485 https://doi.org/10.1006/jssc.1998.7997

[7] T. YOUSEFI, H. R. MAHMUDIAN, M. TORAB-MOSTAEDI, M. A. MOOSAVIAN, R. DAVARKHAH, ANCHOR ING OF CoHFC NANOPARTICLES ON CLINOPTILOLITE FOR REMEDY OF NUCLEAR WASTES, Nuclear Technology & Radiation Protection: 32 (1) (2017) 25-36. https://doi.org/10.2298/NTRP1701025Y

[8] J. X. Li, S. Y. Chen, G. D. Sheng, J. Hu, X. L. Tan, X. K. Wang, Effect of Surfactants on Pb(II) adsorption from aqueous solutions using oxidized multiwall carbon nanotubes,
Chem. Eng. J. 166 (2011) 551-558. [9] Y. K. Zhang, T. Yan, L. G. Yan, X.Y. Guo, L. M. Cui, Q. Wei, B. Du, Preparation of novel
cobalt ferrite/chitosan grafted with graphene composite as effective adsorbents for
mercury ions, J. Mol. Liq. 198 (2014) 381-387. https://doi.org/10.1016/j.molliq.2014.07.043

[10] C. N. R. Rao, A.K. Sood, K.S. Subrahmanyam, A. Govindaraj, Graphene: the new twodimensionalnanomaterial, Angew. Chem. Int. Ed. 48 (2009) 7752-7777. https://doi.org/10.1002/anie.200901678

[11] M. J. Lu, J. Li, X. Y. Yang, C. A. Zhang, J. Yang, H. Hu, X.B. Wang, Applications of
graphene-based materials in environmental protection and detection, Chin. Sci.
Bull. 58 (2013) 2698-2710. https://doi.org/10.1007/s11434-013-5887-y

[12] T. H. Liu, Y. H. Li, Q. J. Du, J.K. Sun, Y. Q. Jiao, G. M. Yang, Z. H. Wang, Y. Z. Xia, W. Zhang,K. L.Wang, H. W. Zhu, D. H. Wu, Adsorption ofmethylene blue from aqueous solution
by graphene, Colloids Surf. B 90 (2012) 197-203. https://doi.org/10.1016/j.colsurfb.2011.10.019

[13] H. Chen, J. X. Li, S. W. Zhang, X.M. Ren, Y.B. Sun, T.Wen, X.K.Wang, Study on the acid-
base surface property of the magnetite graphene oxide and its usage for the removal
of radiostrontium from aqueous solution, Radiochim. Acta 101 (2013) 785-794. https://doi.org/10.1524/ract.2013.2099

[14] Y. G. Zhao, J. X. Li, S. W. Zhang, H. Chen, D. D. Shao, Efficient enrichment of
uranium(VI) on amidoximated magnetite/grapheneoxide composites, RSC Adv. 3
(2013) 18952-18959.

[15] S. W. Zhang, M. Y. Zeng, W. Q. Xu, J.X. Li, J. Li, J.X. Zhang, X.K.Wang, Polyaniline nanorodsdotted on graphene oxide nanosheets as a novel super adsorbent for Cr(VI),
Dalton Trans. 42 (2013) 7854-7858. https://doi.org/10.1039/c3dt50149c

[16] N. Pan, J. G. Deng, D. B. Guan, Y. D. Jin, C .Q. Xia, Adsorption characteristics of Th(IV)
ions on reduced graphene oxide from aqueous solutions, Appl. Surf. Sci. 287
(2013) 478-483.

[17] Z. Yakun, Y. Liangguo, X. Weiying, G. Xiaoyao, C. Limei, G. Liang, W. Qin, D. Bin,
Adsorption of Pb(II) and Hg(II) from aqueous solution using magnetic CoFe2O4-
reduced graphene oxide, J. Mol. Liq. 191 (2014) 177-182. https://doi.org/10.1016/j.molliq.2013.12.015

[18] D. D. Shao, G.S. Hou, J. X. Li, T. Wen, X. M. Ren, X.K.

Wang, PANI/GO as a super
adsorbent for the selective adsorption of uranium(VI), Chem. Eng. J. 255 (2014) https://doi.org/10.1016/j.cej.2014.06.063
604-612.
[19] D. R. Dreyer, et al., The chemistry of graphene oxide. Chemical Society Reviews, 39(1) (2010) 228-240. https://doi.org/10.1039/B917103G
[20] D. C.Marcano , et al., Improved synthesis of graphene oxide. ACS nano, 2010. 4(8): p. 4806-4814. https://doi.org/10.1021/nn1006368
[21] B. Paulchamy, G. Arthi, B. D. Lignesh, A Simple Approach to Stepwise Synthesis of Graphene Oxide Nanomaterial, Paulchamy et al., J Nanomed Nanotechnol 6(2015) 1
DOI: 10.4172/2157-7439.1000253 https://doi.org/10.4172/2157-7439.1000253
[22] Y. Jun Yang, Y. Li, X. Ding, C. Zhang, H. Ren, F. Guo, J.Dong, Synthesis of nickel hexacyanoferrate nanostructure on carbon cloth with predeposited nickel nanoparticles as precursor for binder-free high-performance supercapacitor electrodes, Journal of Alloys and Compounds 871 (2021) 159510. https://doi.org/10.1016/j.jallcom.2021.159510
[23] Y. Seo , Y. Hwang, Prussian blue immobilized on covalent organic polymer-grafted granular activated carbon for cesium adsorption from water, Journal of Environmental Chemical Engineering 9 (2021) 105950 https://doi.org/10.1016/j.jece.2021.105950
[24] F. Ardestani, A. Haghighi Asl, T. Yousefi, M. Torab-Mostaedi, Impregnated of C6CoFeN6 nanoparticles in poly-1- naphthol for uptake of Cs(I) from aqueous, separation Science and technology, 54 (6)(2019)860-875. https://doi.org/10.1080/01496395.2018.1521425
[25] T. Yousefi, M.Torab-Mostaedi, M.A. Moosavian, H. Ghasemi Mobtaker, Potential application of a nanocomposite: HCNFe@ polymer for effective removal of Cs (I) from nuclear waste, Progress in Nuclear Energy 85 (2015) 631-639. https://doi.org/10.1016/j.pnucene.2015.08.006
[26] S. Khandaker, Y. Toyoharaa, S, Kamida, T. Kuba, Adsorptive removal of cesium from aqueous solution using oxidized bamboo charcoal, Water Resources and Industry, 19(2018) 35-46. https://doi.org/10.1016/j.wri.2018.01.001
[27] Yousefi, T., et al., Cerium(III) Molybdate Nanoparticles: Synthesis, Characterization and Radionuclides Ad sorption Studies, Journal of Hazardous Materials, 215-216 (2012), May, pp. 266-271. https://doi.org/10.1016/j.jhazmat.2012.02.064
[28] Y.Zong, Y.Zhang, X.Lin, D.Ye, D.Qiao, S.Zeng, Facile synthesis of potassium copper ferrocyanide composite particles for selective cesium removal from wastewater in the batch and continuous processes, RSC Adv., 7(2017) 31352-31364 https://doi.org/10.1039/C7RA03111D
[29] A. E. Ofomaja, Bioresource. Technol. 101 (2010) 5868-5876. https://doi.org/10.1016/j.biortech.2009.10.064 https://doi.org/10.1016/j.biortech.2010.03.033
[30] M. Sarkar, A. Banerjee, P.P. Pramanick, Ind. Eng. Chem. Res. 45 (2006) 5920-5927. https://doi.org/10.1021/ie060016j
[31] T. Yousefi, S. Yavarpour, S. H. Mousavi, M. Torab-Mostaedi, R. Davarkhah, H. Ghasemi Mobtaker, Process Saf. Environ. 98 (2015) 211-220. https://doi.org/10.1016/j.psep.2015.07.011
[32] C. Aharoni, M. Ungarish, J. Chem. Soc. Faraday Trans. 73 (1977) 456-464. https://doi.org/10.1039/f19777300456 https://doi.org/10.1039/f19777301943